Journal of Materials Chemistry B

ROYAL SOCIETY OF CHEMISTRY

PAPER

View Article Online
View Journal | View Issue

Cite this: J. Mater. Chem. B, 2024, 12, 1558

Pre-formulation of an additive combination of two antimicrobial agents, clofazimine and nisin A, to boost antimicrobial activity†

Mateo Flores Naranjo, Ajay Kumar, Poonam Ratrey and Sarah P. Hudson *

According to the World Health Organization, antimicrobial resistance is one of the top ten issues that pose a major threat to humanity. The lack of investment by the pharmaceutical industry has meant fewer novel antimicrobial agents are in development, exacerbating the problem. Emerging drug design strategies are exploring the repurposing of existing drugs and the utilization of novel drug candidates, like antimicrobial peptides, to combat drug resistance. This proactive approach is crucial in fighting global health threats. In this study, an additive combination of a repurposed anti-leprosy drug, clofazimine, and an antimicrobial peptide, nisin A, are preformulated using liquid antisolvent precipitation to generate a stable amorphous, ionized nanoparticle system to boost antimicrobial activity. The nanotechnology aims to improve the physicochemical properties of the inherently poorly water-soluble clofazimine molecules while also harnessing the previously unreported additive effect of clofazimine and nisin A. The approach transformed clofazimine into a more water-soluble salt, yielding amorphous nanoparticles stabilized by the antimicrobial peptide; and combined the two drugs into a more soluble and more active formulation. Blending pre-formulation strategies like amorphization, salt formation, and nanosizing to improve the inherent low aqueous solubility of drugs can open many new possibilities for the design of new antimicrobial agents. This fusion of pre-formulation technologies in combination with the multi-hurdle approach of selecting drugs with different effects on microbes could be key in the design platform of new antibiotics in the fight against antimicrobial resistance.

Received 9th August 2023,
Accepted 14th January 2024

DOI: 10.1039/d3tb01800h

rsc.li/materials-b

Introduction

The emerging threat that antimicrobial resistance poses to the stability of the global healthcare system has forced the World Health Organization to list the issue as one of the ten biggest threats that currently confront humanity.[1] Beyond the mainstream known causes of antimicrobial resistance, such as the misuse of antibiotics in the medical and food industry, among others,[2] the lack of development of novel drugs and treatments is compromising all the efforts taken to address this issue.[3] The thinning of investment in the development of new antibiotics is not unexpected. The development of new antibiotics has a high failure rate and an elevated cost of production,[4] and with the constant spreading of multi-resistant organisms, the effective lifetime of antimicrobial drugs is continuously shrinking.[5] Novel drugs are still ascertained as last-resort medicines which incur low profitability, thus large companies abandon the market leaving future access to effective antibiotics in jeopardy.[6] Given the high cost of development and manufacture and low investment in antibiotics production, a good strategy to tackle the sluggish pace of drug discovery is the repurposing of existing drugs. This approach can reduce the duration of their development with lower overall development costs and less time-consuming approval processes.[7]

Clofazimine (CFZ) is a riminophenazine dye used in combination with other drugs to treat leprosy. Its efficacy against leprosy was first reported in 1962.[8] Its' mechanism of action is believed to be that it interferes with the electron transport chain in bacteria. It acts as an oxygen-yielding redox species that prompts a new pathway for the NADH electron to exit the respiratory chain.[9] It was formulated in a soft gelatin capsule presentation, and each capsule contained 100 mg of micronized clofazimine suspended in an oil-wax base. This formulation

Department of Chemical Sciences, SSPC, Science Foundation Ireland Research Centre for Pharmaceuticals, Bernal Institute, University of Limerick, Castletroy, Limerick, V94 T9PX, Ireland. E-mail: sarahhudson@ul.ie

† Electronic supplementary information (ESI) available: Table S1 list of conditions screened for preparation of CFZ nanoparticles by liquid antisolvent precipitation. Fig. S1 CFZ TFA nanoparticles size stability over time. Fig. S2 CFZ antisolvent precipitation in 0.1% TFA no stabilizers control over time. Fig. S3 micron-sized CFZ TFA salt particle size distribution. Fig. S4 CFZ TFA, CFZ precipitated in water and CFZ FII complete FTIR spectra. Fig. S5 ^{13}C CPMAS SSNMR spectra of CFZ species and nisin A. See DOI: **https://doi.org/10.1039/d3tb01800h**

resulted in the absorption of up to 70% of the drug compared to less than 20% when it was administered as a crystalline drug.[10]

The main concern due to the low solubility of this drug is achieving enough bioavailability to remain active against its target organisms. Due to the weak basic nature of clofazimine, it can ionize when in the presence of an acidic counterpart and form an ionic salt. The salt formation approach to improving the physicochemical characteristics of clofazimine has been explored for both oral and parenteral delivery, yielding different clofazimine salts with a wide assortment of aqueous solubilities and antimicrobial activities.[11,12]

The commercial clofazimine formulation that was used against leprosy helped several thousands of patients, yet it also yielded several side effects including skin pigmentation, and abdominal pain, among others.[13] However, some studies showed that administering a clofazimine hydrochloride salt reduces the incidence of such side effects compared with clofazimine in its base form.[14] Lately, clofazimine has been repurposed to be used as an anti-tubercular agent as its mechanism of action is believed to be effective against *Mycobacterium tuberculosis* as Mycobacterium species involve an NDH-2 oxidoreductase in their respiratory chain which has a high affinity for CFZ.[9,15]

Other promising molecules to resolve the scarcity of novel antibiotics are antimicrobial peptides. These have been considered as alternative antibiotics due to their promising properties and lower incidence of resistance, but they come with complexities associated with their formulation.[16] Nisin is an antimicrobial peptide produced by *Lactococcus lactis*. This peptide has been used for nearly 50 years as an FDA-approved food preservative and with a lower level of cross-resistance incidence in comparison to standard antibiotics.[17] It is soluble in aqueous media at low pH (1–3) where it adopts a random coil conformation that improves its solubility and interaction with its target in bacteria.[18,19] It has potential use as a therapeutic agent against bacterial infections thanks to its broad-spectrum antimicrobial activity and non-toxicity to humans, and also because of its widely reported synergistic relations with other antimicrobial molecules, Table 1.[20] The mechanism of action of nisin has been widely studied. The peptide breaks down the bacterial membrane by attaching to the precursor lipid II causing efflux of metabolites that permeate the membrane leading to cell death. The nisin-lipid II complex also causes impairment in the cell wall synthesis.[21]

Many formulation strategies have been used to formulate nisin as a potential novel antibiotic promoting better performance and sustained biological activity against a wide range of Gram-positive organisms.[22–24] Previous work from our group attempted to formulate nisin in mesoporous silica matrices, achieving protection from enzymatic degradation and retaining its antimicrobial activity.[25] Similarly, an injectable polysaccharide hydrogel loaded with nisin, and chitosan showed a controlled drug release and synergistic antimicrobial activity against *Staphylococcus aureus*.[26]

Due to the ability of nisin to permeate the bacterial membrane, it is hypothesized that the action of CFZ could be enhanced by the presence of nisin as it will allow CFZ to easily penetrate the bacterial membrane and reach its intracellular targets easier.[9,21] Clofazimine is inherently poorly soluble in water but by salt formation, amorphisation and nanosizing, it's solubility in physiological media can be enhanced. However, nanoparticles are inherently unstable due to agglomeration and Ostwald ripening. Thus in this work, the cationic and polymeric nature of nisin was used to stabilise the clofazimine nanoparticles, resulting in the mixing of clofazimine and nisin on a molecular level in the formulation to enhance the antimicrobial multi-hurdle effect of this drug combination. A combinatorial formulation approach, using clofazimine and nisin, is designed as an important strategy for dealing with antimicrobial resistance. Here, the complementary but different mechanisms of action of the two antimicrobial agents against bacteria can potentially decelerate the development of resistance.[27] Similarly, the use of combinatorial formulation approaches where the components mutually enhance their physicochemical properties can lead to enhanced bioavailability and efficacy.

Table 1 A non-exhaustive list of combinations of nisin with other antimicrobial agents, their level of synergism, and their target organisms

Antimicrobial agent	Target organism	Synergism with nisin	Ref.
Ceftriaxone Cefotaxime	*Salmonella* sp.	Synergistic	29
Ampicillin EDTA	*Salmonella* sp.	Additive	29
Ciprofloxacin Vancomycin	*Staphylococcus aureus*	Synergistic	30
Carvacrol	*Staphylococcus aureus*	Synergistic	31
Ramoplanin	Methicillin-resistant *Staphylococcus aureus*	Synergistic	32
Chloramphenicol Ramplanin	Vancomycin-resistant *Enterococci*	Synergistic	32
Bacitracin	Vancomycin-resistant *Enterococci*	Synergistic	32
Cefazolin	*Staphylococcus aureus* *Enterococcus faecalis*	Synergistic	33
	Staphylococcus intermedius, *Streptococcus agalactiae*, *Streptococcus dysgalactiae*, *Escherichia coli*	Additive	

This can result in a lower dose requirement which can also decrease any potent side effects.[28]

Materials & methods

Materials

Ultrapure Nisin A (95% by *Lactococcus lactis* from sauerkraut) was provided by Handary, Belgium. Clofazimine (CAS registry number 2030-63-9) was provided by Beijing Mesochem Technology Co., Ltd. *Staphylococcus aureus* DSM 20231 strain was received from the DSMZ – German Collection of Microorganisms and Cell Cultures GmbH. The following reagents were purchased from Merck Ireland Ltd and were all used as received: brain heart infusion (BHI) broth, hydrochloric acid (HCl) (37%), lecithin (L-α, from soybean), phosphate-buffered saline (PBS) (tablets), Pluronic F-127 (powder, suitable for cell culture), polyvinyl alcohol (89–99 kDa, 99% hydrolyzed), polyvinylpyrrolidone (40 kDa), potassium chloride (KCl) (99%), tetrahydrofuran (THF) (inhibitor-free, suitable for HPLC, ≥99.9%) and trifluoroacetic acid (TFA) (suitable for HPLC, ≥99.0%).

Experimental methods

Fabrication of solid drug clofazimine TFA salt nanosuspensions stabilized by nisin A

Particles of a clofazimine salt were produced by a liquid antisolvent (LAS) precipitation method. The CFZ solution was prepared by dissolving clofazimine in THF to a concentration of 50 mg mL^{-1}. The following process parameters for the liquid antisolvent precipitation method were screened to select the optimal conditions for the fabrication method: antisolvent composition, solvent–antisolvent ratio, the addition of stabilizing polymers, and CFZ and nisin A concentrations (Table S1, ESI†). The optimized fabrication method involved the injection of 0.3 mL of 50 mg mL^{-1} clofazimine solution in THF into 20 mL of an antisolvent solution, 0.1% v/v TFA (aq.) with 0.4% w/v nisin A as a stabilizer, with magnetic stirring (800 rpm) at 25 °C. Suspensions were also prepared just in 0.1% v/v TFA (aq.) without any nisin A. A complete list of process parameters tested during screening are provided in supplementary information (Table S1, ESI†).

Fabrication of crystalline micron-sized CFZ TFA salt

The crystalline micron-sized CFZ TFA salt was produced using liquid antisolvent precipitation with 100 mL 1 M TFA (aqueous) as antisolvent and a volume of 1 mL of 250 mg mL^{-1} CFZ dissolved in THF under magnetic stirring at 300 rpm and 25 °C. The sample was left stirring for 24 hours and filtered under vacuum through a 0.2 μm pore size nylon membrane. The sample was left drying in an oven overnight at 60 °C and stored at room temperature for further characterization.

Drying of clofazimine TFA salt nanoparticles stabilized by nisin A

The clofazimine TFA salt nanoparticles were freeze-dried immediately after fabrication. To find the ideal concentration of mannitol as a bulking agent, a range of concentrations from 0.1% to 3% w/v were tested. The ideal concentration was found to be 1.5% w/v (1 : 20 weight ratio, CFZ:mannitol). The CFZ nanosuspension with the corresponding amount of mannitol was frozen at −80 °C for 2 hours before freeze-drying. The lyophilization process was done on a TelStar lyoquest freeze dryer at −80 °C with vacuum. The nanoparticle powder was subsequently stored at room temperature.

Particle size and zeta potential analysis

The particle size distribution and zeta potential of the nanosuspension were measured by dynamic light scattering (DLS) using a Malvern Zetasizer Nano. For size analysis, aliquots of the different suspensions were added to disposable cuvettes and measured at a detection angle of 173° and 25 °C in triplicate. For zeta potential analysis, aliquots of different suspensions were added to disposable capillary cells and determined from electrophoretic mobility by using the Smoluchowski approximation.

The particle size distribution of the micron-sized CFZ TFA salt was determined using a Malvern Mastersizer 3000 with water as the dispersant. The parameters used for the sample analysis were an obscuration rate of 2% to 8%, a stirring rate of 1500 rpm, and a premeasurement delay of 10 s. The refractive index of clofazimine was set at 1.67 and the absorption index at 0.01. Three measurements were conducted per run and the sample was analyzed in triplicate using independent resuspended samples. The particle size is reported as D10, D50 or D90 values which represent the particle size that 10%, 50% or 90% of the particles present are smaller than.[34]

Powder X-ray diffraction (PXRD)

Reflection powder X-Ray diffractograms (PXRD) were obtained with an Empyrean X-Ray diffractometer (PANalytical, Phillips) with Cu Kα1,2 radiation (λ = 1.5406 Å) operating at 40 kV and 40 mA at room temperature. All samples were scanned from 5 to 50° 2θ with 0.0026° 2θ per min steps and 112.97 s per step, on a flat surface spinning at 4 rpm.[17] The diffractograms for the base forms of clofazimine and previously reported CFZ salts were obtained from the Cambridge Structural Database (CSD).[35]

Fourier-transform infrared spectroscopy (FTIR)

The samples were prepared using the same conditions as for the fabrication of nanoparticles, injecting 0.3 mL of a 50 mg mL^{-1} CFZ solution in THF to 20 mL of the antisolvent, 0.1% TFA (aq.) or Di-H_2O respectively to compare the effect of the acid antisolvent in the protonation state of CFZ after precipitation. No nisin A was present during these preparations and the resulting microparticles were filtered using a Buchner funnel and dried under ambient conditions. Fourier-transform infrared (FTIR) spectra of the dried powders were collected on a Thermo Scientific Nicolet iS50 FTIR spectrometer equipped with a diamond ATR accessory. Spectra were collected at room temperature with an average of 128 scans and a resolution of 2 cm^{-1} in the spectral region from wavenumber 4000 to 650 cm^{-1}.

Solid-state state nuclear magnetic resonance (SSNMR)

^{13}C CPMAS solid-state nuclear magnetic resonance spectra were collected on a Bruker Avance III HD NMR spectrometer operating at a 9.4 T magnetic field with ^{1}H and ^{13}C resonance frequencies of 400.1 and 100.6 MHz respectively. CFZ FII (starting material), crystalline micron-sized CFZ TFA salt, nisin A, and freeze-dried CFZ TFA salt nanoparticles stabilized by nisin A were packed in 4 mm zirconia rotors under ambient conditions and capped. ^{13}C CPMAS NMR spectra were acquired at natural abundance with a double resonance triple channel 4 mm Bruker MAS probe. The spectra were referenced by setting the high frequency ^{13}C resonance of adamantane to 38.48 ppm. The spectra were acquired using a cross-polarization pulse with a magic-angle spinning rotor frequency of 10 KHz. The acquisition parameters were optimized to a contact time of 4.5 ms and a relaxation delay of 3.58 s, with 500 scans collected for micron-sized CFZ TFA salt and nisin A, and 2000 scans collected for the CFZ TFA nanoparticles stabilized with nisin A.

Dissolution studies

Dissolution tests of CFZ FII (starting material), the fresh CFZ TFA nanosuspension stabilized by nisin A, and freeze-dried CFZ TFA nanoparticles stabilized by nisin A were conducted under non-sink conditions with a maximum clofazimine solution concentration of 50 mg L^{-1} in deionized water at 37 °C and 300 rpm continuous agitation. The drug concentration was measured using a Shimadzu UV-1800 UV-vis spectrophotometer at a detection wavelength of 488 nm. For calibration of the instrument, standard CFZ solutions were made in THF with a concentration range from 0.1–20 mg L^{-1} with a linear factor R^2 = 0.9999.

Minimum inhibitory concentration (MIC) determination against *S. aureus*

The minimum inhibitory concentrations of both CFZ and nisin A were assessed following the Clinical and Laboratory Standards Institute guidelines for antimicrobial susceptibility determination.[36] Briefly, an overnight culture of *Staphylococcus aureus* DSM 20231 was grown in a BHI agar plate. Three colonies of similar morphology were resuspended and diluted in BHI broth to reach an optical density (OD) of 0.1 at 595 nm wavelength. The culture was further diluted just before use so the bacterial concentration in the 96-well microplate was 10^5 CFU mL^{-1}. A volume of 99 μL of the diluted bacterial cell culture was added to a 96-well microplate.

Then, 1 μL of clofazimine or nisin A solutions were added (n = 5) to reach a final volume of 100 μL at different drug concentrations. Blanks of PBS with media only and each concentration of clofazimine solution with media only were set up. A negative control was set up with bacterial culture and PBS buffer (n = 5). The 96-well plate was incubated at 37 °C for 24 hours with optical density readings every 30 minutes at a wavelength of 595 nm, in a Biotek ELX808 Ultra microplate reader. The drug solutions tested were made in THF for CFZ, and 0.1% TFA (aq.) for nisin A. 1 μL of each solvent system were tested to ensure no activity was exerted by the solvent systems.

Also, suspensions of both drugs in PBS were tested to confirm the need for THF and 0.1% TFA to dissolve CFZ and nisin A respectively to enable antimicrobial activity.

Synergy of combinations of clofazimine and nisin A

The synergy between clofazimine and nisin A was tested using fractional inhibitory concentration (FIC) indexes. FIC index analysis was performed following the checkerboard method.[37] The *S. aureus* culture was prepared as described in the previous section. 98 μL of bacterial cell culture was added to a 96-well microplate. Then, 1 μL of a clofazimine solution and 1 μL of a nisin A solution at the desired concentration were added to fill in the checkerboard (2 μL PBS was used for the starting point). The 96-well plate was incubated for 24 hours at 37 °C. Optical density was measured after 24 hours in a Biotek ELX808 Ultra microplate reader. Minimum inhibitory concentrations were determined as those in wells that showed less than 10% growth compared to the positive control (2 μL PBS or 0 μg mL^{-1} of clofazimine and nisin in the checkerboard). FIC indexes were determined by the following equation, where the concentration of clofazimine in the well is divided by its MIC alone plus the concentration of nisin in the well divided by its MIC alone determined in the previous section.

$$\mathrm{FICI} = \frac{\mathrm{Conc_{CFZ}}}{\mathrm{MIC_{CFZ}}} + \frac{\mathrm{Conc_{nisin}}}{\mathrm{MIC_{nisin}}} \quad (1)$$

Antibacterial activity by total plate counts

The *S. aureus* culture was prepared as described above. 98 μL of bacterial cell culture were added to a 96-well microplate. 1 μL of PBS was added when only one drug alone was tested. The solutions of CFZ TFA nanosuspension and nisin A were diluted with 0.1% TFA and CFZ with THF, to the concentrations needed.

Then, 1 μL of diluted CFZ TFA nanosuspension, clofazimine FII, and nisin A solutions and combinations were added to reach a final volume of 100 μL and incubated for 3 hours at 37 °C. The content of each well was diluted with PBS buffer by decimal dilution factors as required. 10 μL of these dilutions were plated on BHI agar Petri dishes and incubated for 18 hours. The negative control was set up using bacterial culture and PBS buffer and was also plated at different dilution factors. A sample of 10 μL was plated for each sample. The colonies were counted and reported as log (CFU mL^{-1}).

Analysis of the morphology of bacterial cells by SEM

An overnight culture of *S. aureus* was prepared as described above. Bacterial cells were incubated with the CFZ TFA nanosuspension and PBS for control cells at 37 °C overnight in a 96-well plate. After incubation, the treated and control cells were centrifuged at 6000 rpm for 2 minutes. The cell pellets were washed thoroughly with PBS buffer and fixed with 2.5% v/v glutaraldehyde in PBS at 37 °C overnight. After fixation, the cell

pellets were washed with PBS buffer and water. The resuspended cells in water were lyophilized to dryness. Finally, the powdered cells were placed onto carbon tape over a metallic scrub and coated with gold for 120 seconds before SEM analysis.[38] Scanning electron microscopy (SEM) was performed on a Hitachi S-U70 scanning electron microscope under a 10 kV operating voltage.

Statistical analysis

One-way ANOVA was used to determine the significant differences between the negative control and the test samples in the colony counting assay. Tukey's test was used for comparison of mean values and Levene's test for comparison of variances at a probability threshold of 0.05. The results are considered significantly different if $p \leq 0.05$ in both comparison tests.

Results and discussion

Production and characterization of clofazimine TFA salt nanoparticles stabilized by nisin A

The low aqueous solubility of clofazimine and the poor solubility of nisin A in pH solutions greater than 2, present a concern for the pharmaceutical formulation of these drugs. Harnessing the differences in solubility of clofazimine and nisin A to produce a pre-formulated system, liquid anti-solvent precipitation (LASP) was used to fabricate clofazimine TFA salt nanoparticles stabilized by nisin A. After screening of different anti-solvents and other polymeric stabilizers together with nisin A (Table S1, ESI†), it was found that 0.4% w/v nisin A in 0.1% v/v TFA (aq.) yielded the most stable nanosuspension (Fig. S1, ESI†).

In previous work from our group, it was shown that, according to the pK_a rule, acid coformers that yield a ΔpK_a value greater than 2 units with CFZ (pK_a = 8.55), will prompt the protonation of CFZ and the formation of a salt with the conjugated base of the respective coformer.[12] Here, the use of TFA (pK_a = 0.23) as an antisolvent yields a ΔpK_a value of 8.32 against CFZ, which would suggest the high probability of the formation of a CFZ TFA salt during the anti-solvent precipitation process. For comparison with the CFZ TFA salt nanosuspensions stabilized by nisin before and after freeze-drying, controls of a crystalline micron-sized CFZ TFA salt powder (produced by liquid anti-solvent precipitation at different conditions in the absence of nisin), CFZ (FII) suspension (produced using water as an anti-solvent in the absence of nisin) and form II clofazimine polymorphic powder (as received) were studied.

The average particle size of the CFZ TFA salt nanosuspension stabilized by nisin A was 180 nm with a polydispersity index of 0.2 and a zeta potential of +27 mV. The nanoparticles showed stability for up to 6 hours in suspension (Fig. S1, ESI†). In comparison, the anti-solvent precipitation of CFZ in 0.1% TFA without the presence of any stabilizers yielded a particle size of 300 nm, PDI of 0.372, and zeta potential of +55 mV initially but grew into visible particles within 10 minutes and precipitated out of solution (Fig. S2, ESI†). The lower zeta potential displayed by the nanosuspension in comparison to CFZ particles produced without any stabilizers, Table S1 (ESI†), may be due to nisin A masking the zeta potential of CFZ. Thus, it is hypothesized that nisin A is deposited on the surface of the solid CFZ TFA salt nanoparticles preventing aggregation, likely, through a steric stabilization mechanism.

After resuspension in DI-H_2O, the prepared crystalline micron-sized CFZ TFA salt powder yielded a particle size range between 8 and 330 μm (Table 2 and Fig S3, ESI†). Immediately after production, the nanosuspension was freeze-dried with mannitol as a cryoprotectant at concentrations ranging from 0.1% to 3% w/v for 48 hours. It was found that below 1.5% w/v mannitol concentration, the lyophilized cake does not resuspend easily, and the powders turn into clumps as soon as the lyophilization process was complete and the powder was exposed to ambient temperature and pressure. Thus, a concentration of 1.5% w/v mannitol was chosen for further studies. After resuspension of the lyophilized CFZ cake in DI-H_2O, the particles displayed an average particle size of 557 nm and PDI of 0.7, indicating the nanoparticles are not stable through the lyophilization process. Similar particle sizes were obtained at higher concentrations of mannitol (Table 2).

To confirm the formation of a new CFZ TFA salt during LAS precipitation, the starting material (CFZ FII polymorph), freeze-dried CFZ TFA salt nanoparticles, and the crystalline micron-sized CFZ TFA salt powder were analyzed by PXRD and compared to calculated diffractograms of the reported CFZ species in the CSD database.[35] It was not possible to directly analyze the CFZ TFA salt nanoparticles stabilized with nisin in suspension by PXRD. The crystalline micron-sized CFZ TFA salt (no nisin present) showed a different diffraction pattern than the starting materials and the reported calculated polymorphic forms of CFZ as well as the other reported salts, suggesting the formation of a novel CFZ TFA salt. The freeze-dried nanoparticles showed peaks corresponding to the δ form of

Table 2 Particle size, PDI, and zeta potential of clofazimine TFA salt particles generated before and after lyophilization

CFZ TFA salt particles	Average particle size	PDI	Zeta potential (mV)
Crystalline CFZ TFA salt (no nisin present)[a]	D10 – 8.44 ± 0.3 μm D50 – 35.6 ± 2.4 μm D90 – 329 ± 31.9 μm	—	—
Fresh nanosuspension (with nisin)[b]	177.4 ± 3.18 nm	0.2 ± 0.01	26.9 ± 1.04
Freeze-dried nanoparticles (with nisin)[b]	557 ± 32.8 nm	0.7 ± 0.02	—

[a] PSD measured on mastersizer immediately after precipitation or resuspension. D10, D50 or D90 sizes are the size below which 10%, 50% or 90% of particles are measured respectively. [b] PSD measured on Zetasizer immediately after precipitation or resuspension.

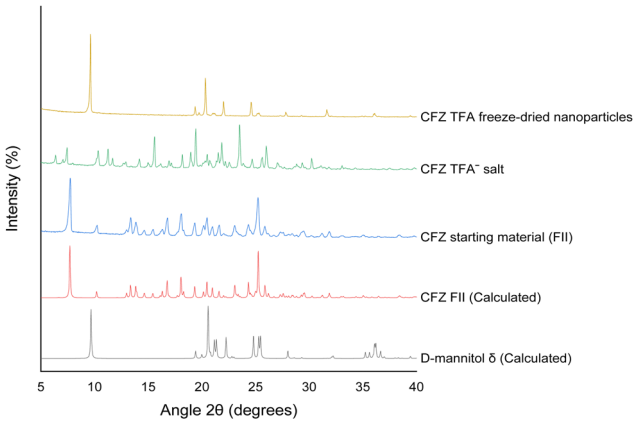

Fig. 1 Comparison of the experimental PXRD diffractograms of CFZ species and excipients including CFZ FII polymorph, freeze-dried CFZ TFA salt nanoparticles with mannitol, the crystalline micron-sized CFZ TFA salt powder with CSD calculated spectra for CFZ FII: DAKXUI and d-mannitol: DMANTL02.

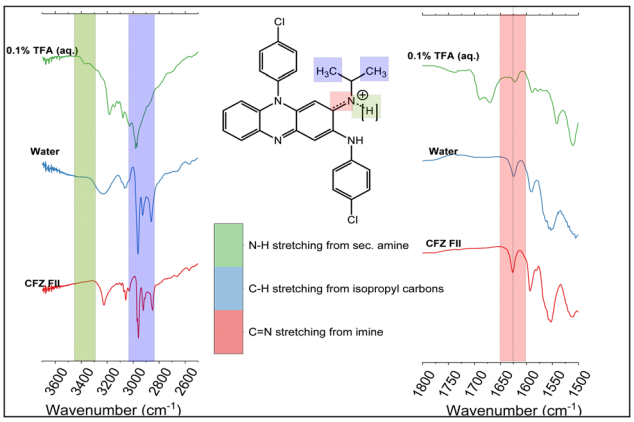

Fig. 2 Segments of the FT-IR spectra of CFZ after liquid antisolvent precipitation in 0.1% TFA and water as antisolvents respectively and compared to the CFZ starting material (FII polymorph). No nisin was present in these samples.

D-mannitol but no other significant diffraction peaks, confirming the amorphous nature of the CFZ TFA salt nanoparticles.

Even so, some very small peaks in the diffractogram of the freeze-dried CFZ TFA nanoparticles are congruent with those of the micron-sized TFA salt, suggesting the transformation to the crystalline salt during fabrication and drying of the nanosuspension. It is hypothesized that during the preparation of the nanosuspension, high supersaturation levels lead to the precipitation of an amorphous form. The presence of nisin as a stabilizer prevents or slows the transformation of CFZ TFA salt to a crystalline form, (Fig. 1). Nonetheless, the analysis of the PXRD diffractograms was inconclusive to confirm the production of the CFZ TFA salt during the production of the nanoparticles stabilized by nisin A, but the CFZ TFA salt material without any stabilizers yielded a diffraction pattern that has not been reported to date, indicating the formation of a novel crystalline material.

To investigate if the CFZ TFA salt was indeed formed during the production of the nanoparticles it was necessary to confirm if CFZ is in a protonated state after precipitation from the solvent/antisolvent mixture. FT-IR spectroscopy and ^{13}C CPMAS SSNMR were used to assess the structural changes of CFZ in the solid state during the production of the nanoparticles. It is clear from the FTIR spectra that when water is used as an antisolvent, the resulting solid is the FII polymorphic form (Fig. 2).

When aqueous 0.1% (w/v) TFA was used as the antisolvent, the shifting of the peak from the ketimine bond around 1650 cm^{-1} towards lower wavenumbers indicates a decrease in the energy of the bond. This is associated with the weakening of the C=N bond due to the protonation of that nitrogen in the acid–base reaction with the acid coformer present in the antisolvent (Fig. 2 in red).[12] A small band at 3500 cm^{-1} is observed in the spectrum of the sample precipitated in 0.1% TFA (aq.). This band corresponds to the new N–H stretching generated by the protonation of the imine group. This band does not appear in either the starting material (CFZ FII) or the sample precipitated in water, indicating protonation in the sample precipitated in 0.1% TFA (aq.) (Fig. 2 in green). Furthermore, it is noted that the bands corresponding to the C–H stretching in the methyl groups in the isopropyl region of the molecule appear to be broadened and overlapped. There are reports that TFA complexes in protonated molecules affect the motility and length of the bonds due to hydrogen bonding, which may explain the effect on the isopropyl bands in the protonated CFZ TFA sample (Fig. 2 in blue).[39]

The SSNMR spectra of nisin alone, CFZ FII, micron-sized CFZ TFA salt, and freeze-dried CFZ TFA nanoparticles with nisin were compared to further prove the formation of the TFA salt during the production of the nanoparticles. Consistent with previous studies,[12] the ketimine and isopropyl carbons (Fig. 3 in red, green respectively) bonded to the imine nitrogen exhibited an up-field shift in both the CFZ TFA salt and the CFZ TFA nanoparticles, compared to the starting material (CFZ FII). These up-field shifts are attributed to electron density being pulled towards the more electronegative nitrogen after protonation. In the case of the isopropyl carbon, the change in chemical shift may be due to electron density migrating from the methyl groups towards the protonated nitrogen causing a shielding effect on the carbon and thus, a shift to lower chemical shift values. Similarly, the electron density migrating from the phenazine nucleus toward the protonated nitrogen generates a shielding effect on the ketimine carbon and an up-field shift in the corresponding peak (Fig. 3 in red).[40] In contrast, the other ketimine carbon within the phenazine ring (Fig. 3 in blue) showed no significant shift upon protonation. The peaks in the SSNMR spectrum of the nanoparticles were broadened due to the amorphous nature of the nanoparticles but they overlaid accurately with both CFZ TFA salt and nisin A spectra. Overall, these results support the hypothesis of the formation of a CFZ TFA salt during the production of nanoparticles stabilized by nisin A by liquid antisolvent precipitation.

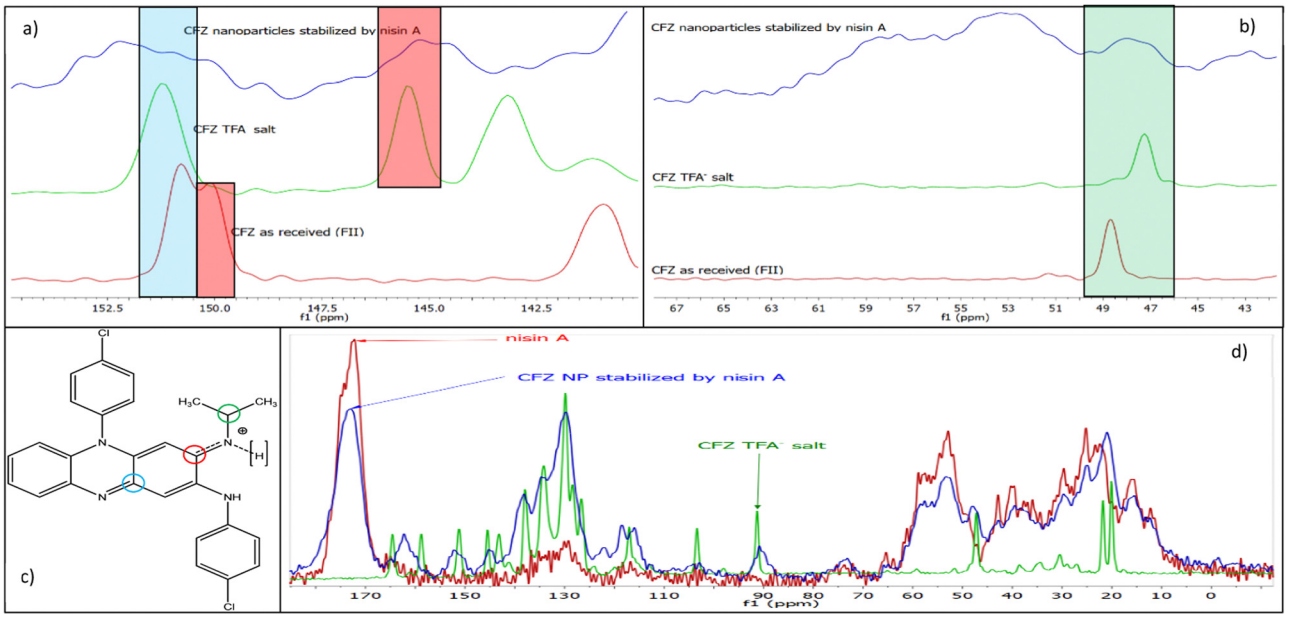

Fig. 3 Comparison of ^{13}C CPMAS SSNMR spectra of CFZ TFA^- nanoparticles (with nisin), micron-sized CFZ TFA^- salt, CFZ FII, and nisin A. (a) Segment of spectra of the chemical shift of ketimine carbons (red and blue). (b) Segment of the spectra of the chemical shift of isopropyl carbon (green). (c) Clofazimine structure. (d) Overlay panel of CFZ TFA^- nanoparticles (with nisin), micron sized CFZ TFA^- salt and nisin A complete ^{13}C CPMAS spectra.

To understand the improvement in the solubility and dissolution rate that can be achieved by the reduction of size, amorphization, and salt formation from the formulation strategy designed in this work, dissolution profiles in water under non-sink conditions were measured for both the fresh CFZ TFA nanosuspension and the freeze-dried CFZ TFA nanoparticles as well as the new micron-sized CFZ TFA salt (Fig. 4). The fresh CFZ TFA nanosuspension showed the fastest dissolution rate and reached the highest concentrations of CFZ in water, with almost 40% of added CFZ dissolving within 10 minutes and maxing out at almost 50% after 30 minutes. The freeze-dried CFZ TFA nanoparticles, in turn, reached a cap of 10% dissolution of added CFZ within 10 minutes. Such a decrease in the maximum solution concentration and dissolution rate might be due to the difference in the particle size which more than doubled upon freeze-drying. The crystalline CFZ TFA salt had an even lower maximum solution concentration after 1 hour compared to the freeze-dried nanoparticles and a much slower dissolution rate. This is attributed to the difference in particle size (Table 2) and crystallinity (Fig. 1).

The CFZ TFA nanosuspension showed 5 times more clofazimine in solution compared to the crystalline micron-sized CFZ TFA powder after 1 hour. Also, the amount of non-ionized CFZ FII (as received) that gets dissolved in DI-H_2O was not detectable (limit of detection was 0.1 mg L^{-1}). Previous studies from our group also showed very poor solubility of CFZ FII in aqueous media.[41] The observed significant improvement in the solution concentration by the amorphous ionized nanoparticles at corporal temperature could be crucial to achieving a better bioavailability of the drug and thus, better pharmacodynamics.

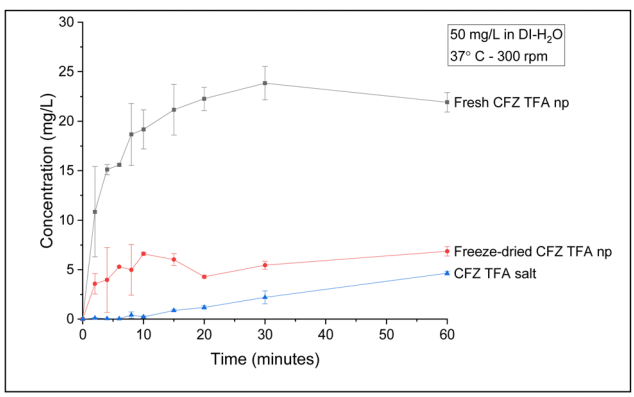

Fig. 4 Comparison of the dissolution profiles of CFZ TFA salt nanoparticles stabilized by nisin A, before and after freeze-drying, and micron-sized CFZ TFA salt in DI-H_2O.

Antimicrobial activity of clofazimine and nisin by themselves and combined.

The minimum inhibitory concentration (MIC90), defined as the lowest concentration necessary to inhibit 90% of the bacterial growth, was determined for both CFZ and nisin A dissolved in THF and 0.1% TFA (aq.) respectively, against *S. aureus*. It was found that 5 μg mL^{-1} CFZ is needed to inhibit bacterial proliferation (Fig. 5a). In turn, 20 μg mL^{-1} nisin A is needed to achieve the same inhibition (Fig. 5b).

It was also found that sub-MIC concentrations of nisin A promote the growth of *S. aureus*, as the bacteria proliferate to higher optical density values at such concentrations in comparison to the negative control. The enhancement of bacterial proliferation by the effect of a drug is referred to in the literature as hormesis. The hormetic effect is a dose–response

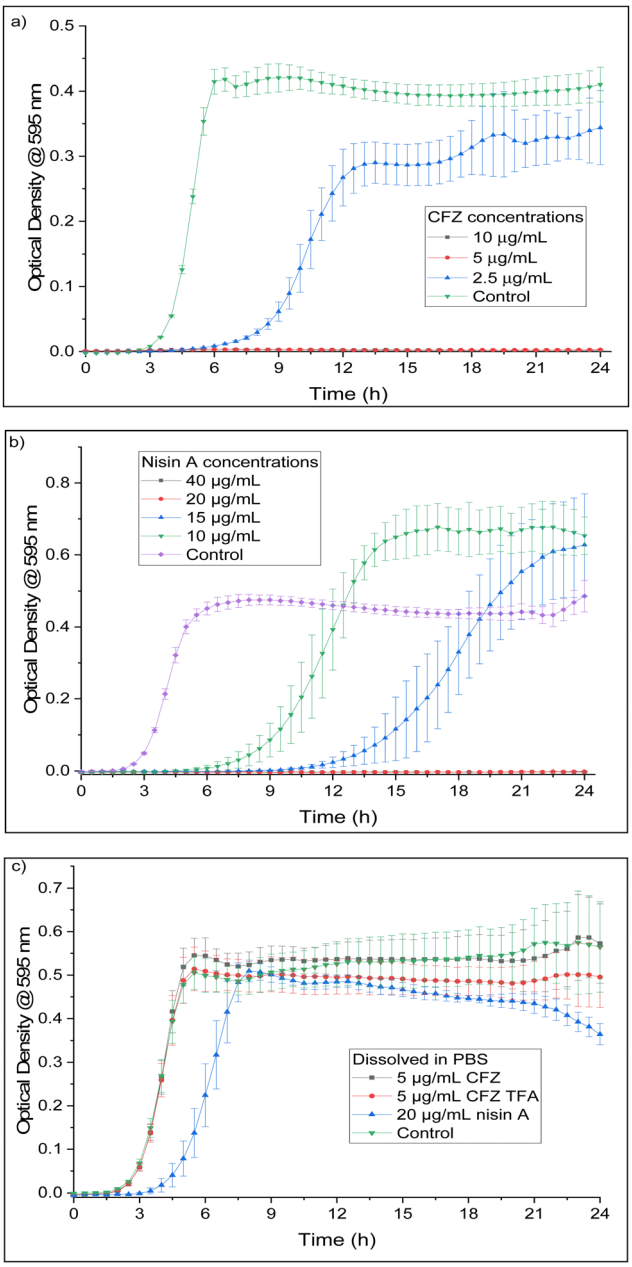

Fig. 5 Growth curve of *S. aureus* after treatment with different concentrations of (a) CFZ dissolved in THF, (b) nisin A dissolved in 0.1% TFA (aq.) and, (c) CFZ FII, micron-sized CFZ TFA salt, and nisin A respectively suspended in PBS. Controls of the respective solvents in each graph are also presented.

adaptive function regarded as a defensive response to low concentrations of stressors.[42] Many antimicrobial peptides have shown a similar effect on their target organisms but there are no reports with mechanistic information on the occurrence of hormesis.[43] The negative control with the respective solvent for each drug was assessed showing no effect of the solvents on the bacterial viability (Fig. 5).

To confirm if the need of organic solvent and acid buffers to attain a solution concentration to uphold the biological activity of the drugs, the MICs of each component were tested using PBS as the dissolution medium following the same procedure as with the dissolved drugs. The same was done with the micron-sized CFZ TFA salt and tested at the same MIC value of 5 μg mL^{-1} as the starting material (CFZ FII). Neither the FII nor the TFA salt showed activity at that concentration with the growing curve looking identical to the negative control. In the case of nisin at 20 μg mL^{-1} in PBS, it showed a small increase in the lag phase of the bacteria and a small decrease in the total growth after 24 hours, which suggests some nisin A can be dissolved in PBS but not enough to achieve proper bioactivity. This result also confirms the low solubility of nisin A in solutions with pH values greater than 2 (Fig. 5c).

The effect of the combination of CFZ and nisin A in THF and 0.1% TFA respectively, was tested in a checkerboard microplate testing 2-fold serial dilution from their respective MIC values. It was found that the combination of concentrations between 15 and 10 μg mL^{-1} nisin A with 0.625 to 2.5 μg mL^{-1} CFZ yielded an inhibition of at least 90% of the growth of *Staphylococcus aureus*. An analysis of the fractional inhibitory concentration indices of the combination of the drugs showed an additive effect between these two drugs (Table 3). During these initial assays to determine the activity of the individual clofazimine and nisin A components and the bioactivity of the combination of these drugs, the addition of organic solvents and acid buffers (1% v/v) was still needed to achieve the desired concentrations in solution and the observed activity. Without the THF organic solvent or the acidic buffer, no activity was observed (Fig. 5c).

In vitro antimicrobial activity of CFZ TFA nanoparticles stabilized by nisin A

The activity of the amorphous CFZ TFA nanoparticles stabilized by nisin A was tested against *S. aureus* by total plate counts. Due to the increased particle size and lower dissolution in water of the freeze-dried nanoparticles, the activity was assessed using the fresh CFZ TFA nanosuspension (Table 1 and Fig. 4). The nanosuspension was diluted in 0.1% TFA (aq.) to meet the range of concentrations at which the combination of both drugs (CFZ FII and nisin A) showed additivity, diluting the amount of THF added to the total experimental volume in the well. After treatment for 3 hours (Fig. 6a), it was found that at ~2.5 μg mL^{-1} CFZ TFA + 13 μg mL^{-1} nisin A of the nanosuspension, the reduction of the growth of *S. aureus* corresponds to 3.5 log reductions or 99.98% inhibition. For comparison, a

Table 3 Fractional inhibitory concentration indices of the combination of CFZ and nisin A against *S. aureus*

Drug combination, incubation time	FICI median (range)	Concentration range nisin A	Concentration range CFZ
CFZ (in THF) + nisin A (in 0.1% TFA), 24 h	1.18 (1–2)	15–10 μg mL^{-1}	2.5–0.625 μg mL^{-1}

combination of CFZ and nisin A previously dissolved in THF and 0.1% TFA (aq.) respectively at the same approximate concentrations were also tested. This showed a comparable activity, being statistically similar to the samples of nanoparticles and statistically different from the negative control. Similarly, ~1.25 μg mL^{-1} CFZ TFA + 6 μg mL^{-1} nisin A of the nanosuspension yielded a decrease of 1.5 log reductions or 97% inhibition of the growth of the bacteria. These were also comparable to the combination of previously dissolved drugs. The samples treated with this combination of previously dissolved drugs were also significantly different to the negative control, but the ones treated with nanoparticles were not, despite being statistically similar to each other.

After 24 hours of treatment (Fig. 6b) with ~2.5 μg mL^{-1} CFZ TFA + 13 μg mL^{-1} nisin A, the nanosuspension reduced the proliferation of *S. aureus* by 2.5 logs in comparison to the negative control. In turn, the combination of previously dissolved drugs at the same approximate concentrations yielded almost 5 log reductions. Despite the large standard deviations of the combination of previously dissolved drugs, it was statistically more active than the samples treated with the nanoparticles. The reduction in the activity of the nanoparticles at these concentrations might have to do with their stability (Fig. S1, ESI†). After 6 hours, the suspension showed large agglomerates and precipitated out of solution, and analysis by DLS was no longer suitable. The inherent low aqueous solubility of these agglomerates might be responsible for their reduced bioactivity over longer periods of time. When treated with ~1.25 μg mL^{-1} CFZ TFA + 6 μg mL^{-1} nisin A of the nanosuspension, the proliferation of *S. aureus* was reduced by 1.5 log reductions. A similar reduction was observed in the samples treated with a combination of previously dissolved drugs at the same concentrations with larger standard deviations. The statistical analysis showed that the samples treated with the previously dissolved drugs were not significantly different to the negative control. In turn, the ones treated with the nanosuspension were statistically different to the negative control and the previously dissolved drugs counterpart, indicating a better performance by the nanoparticles at these concentrations achieving a reduction of 97% of the proliferation of the bacteria.

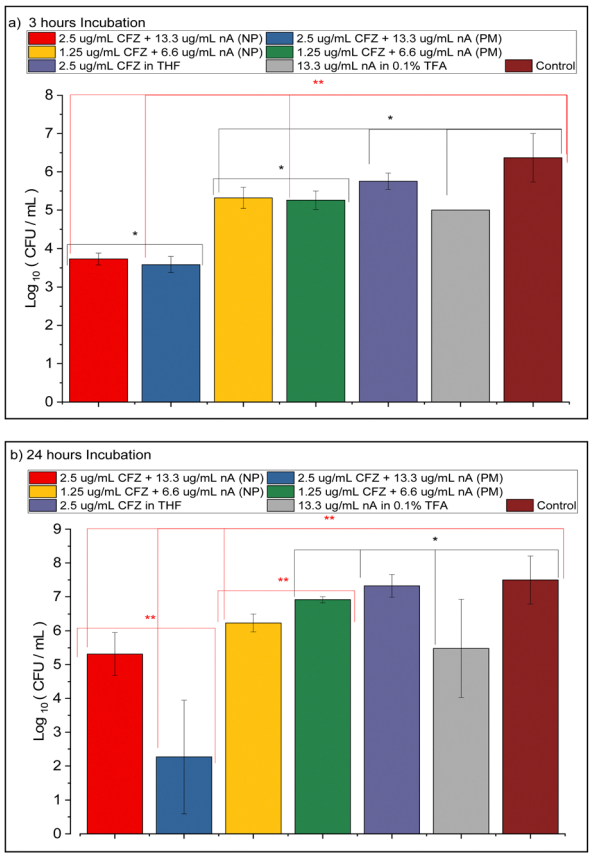

Fig. 6 Colony counts of *S. aureus* after (a) 3 hours and (b) 24 hours treatment with different concentrations of fresh CFZ TFA salt nanosuspensions stabilized by nisin A and solutions of each drug alone and in combination with each other, CFZ FII and nisin A (nA) in THF and 0.1% TFA respectively. The concentrations shown are in μg mL^{-1}. * population not significantly different at 0.05 confidence level. ** population significantly different at 0.05 confidence level. Abbreviations: NP: nanoparticles, PM: physical mix of previously dissolved drugs.

The performance of CFZ in THF at 2.5 μg mL^{-1} or nisin A in 0.1% TFA (aq.) at 13.3 μg mL^{-1} alone were not significantly different to the negative control at both 3 and 24-hour treatment. The nanosuspension was diluted with 0.1% TFA to achieve the desired concentrations. Therefore, volumes of up to 10 μL of 0.1% TFA (aq.) were tested as a negative control and showed no activity against *S. aureus*. It should be noted that the wells treated with the CFZ TFA nanosuspensions stabilized by nisin A, had less than 0.0005% of THF due to dilution to meet the desired concentrations compared to the ones treated with individual previously dissolved solutions of CFZ in THF, with and without nisin, where 1% THF was present in the total volume of the wells.

Despite this significant reduction in solvent content (by a factor of ~1000), activity is retained in the nanosuspension at approximately the same concentrations of CFZ and nisin A previously dissolved in their preferred solvents. Given that no activity was observed in PBS and in the absence of any organic solvent (Fig. 5c), these results show promise for improved bioavailability and *in vivo* antimicrobial activity of the drugs upon administration to the body. The reduction in size, salt formation, and amorphization play a crucial role in achieving this boosted antimicrobial activity.

The effect of nanoparticles on the morphology of the bacterial membrane

Nisin A acts on bacteria by attaching to the lipid II precursor and disrupting the biosynthesis of the cell membrane.[31] The proposed mechanism of action of CFZ suggests that it disrupts the bacterial respiratory chain and binds to bacterial DNA preventing cell division and promoting cell death.[15] It is then hypothesized that the additive mechanism between nisin A and CFZ lies on the permeation of the membrane by the effect of nisin A, thus facilitating the translocation of CFZ inside the cell facilitating its mechanism of action. The effect of the

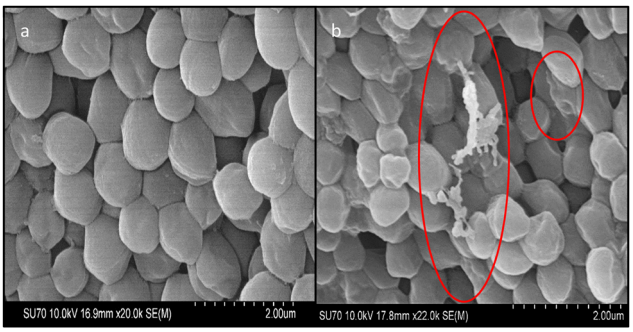

Fig. 7 SEM micrographs of *S. aureus* (a) control cells, and after treatment with (b) CFZ TFA salt nanoparticles both containing approximately 1.25 μg mL^{-1} CFZ + 13.33 μg mL^{-1} nisin A.

formulation in the bacterial membrane is analyzed by SEM micrographs after treatment with the drugs. The control cells (Fig. 7a) showed the expected morphology of *S. aureus*, round cells. The cells present some dents in the bacterial membrane that are attributed to defects and dehydration generated by the processing of the cells before SEM analysis. In turn, the cells treated with the CFZ TFA nanosuspension showed major defects in the morphology of the bacteria. The micrograph showed bacterial cells with major punctures and cellular content leaking from such (Fig. 7b). The activity of the nanoparticles correlates with the augmented interaction and effect on the stability of the bacterial membrane.

Conclusions

This study has revealed that CFZ can be formulated as solid drug nanoparticles stabilized by nisin A. The use of liquid antisolvent precipitation with 0.1% TFA (aq.) as anti-solvent to produce the nanoparticles yielded the formation of a novel CFZ TFA salt. The incorporation of nisin A as a stabilizer prevents the transformation of the salt to a crystalline form, generating amorphous nanoparticles. The nanosuspension of CFZ TFA stabilized by nisin A, and the novel CFZ TFA crystalline salt exhibits a higher water solubility than CFZ in its base form. Similarly, the CFZ TFA nanosuspension stabilized by nisin A achieved a higher solution concentration and faster dissolution rate compared to the micron-sized crystalline CFZ TFA salt. Finally, the nanosuspension showed comparable activity to a combination of CFZ and nisin A previously dissolved in THF and 0.1% TFA (aq.) respectively using a 1000 times lower solvent content. The nanosuspension had a pronounced impact on the morphology of the bacterial membrane. A multi-hurdle, multi-drug approach is a useful tool in the race against antimicrobial resistance. However, combining it with other pre-formulation strategies, such as amorphization, size reduction, and salt formation, improves the dissolution behaviour of poorly water-soluble existing drugs and can further boost antimicrobial activity. The combinatorial formulation of CFZ and nisin A showed an improvement in the bioactivity of the drugs against *S. aureus*. Nisin A showed an inherent ability to stabilize amorphous CFZ TFA nanoparticles while at the same time strengthening their effect against bacteria. Furthermore, the utilization of liquid antisolvent precipitation with acidic anti-solvents as a platform for the fabrication of different CFZ salt nanoparticles unlocks the possibilities to modulate the solubility and dissolution rate of CFZ towards more aqueous soluble species. It was previously reported that salt forms of CFZ can retain their biological activity while reducing its side effects. However, the blend of strategies like amorphization, salt formation, and nanosizing to improve the inherent low aqueous solubility of CFZ, reducing the concentration of drug needed to achieve the same biological activity, which can be positive for the reduction of undesired side effects.[14] Similarly, the combination of molecules with different effects on microbes merging with various pre-formulation strategies can be key in the design platform of new antibiotics in the fight against antimicrobial resistance.

Author contributions

Mateo Flores Naranjo: conceptualization, methodology, investigation, validation, formal analysis, data curation, visualization, writing – original draft. Ajay Kumar: methodology, investigation, supervision. Poonam Ratrey: methodology. Sarah P. Hudson: conceptualization, resources, writing – review & editing, supervision, project administration, funding acquisition.

Conflicts of interest

There are no conflicts to declare.

Acknowledgements

The work reported in this publication is supported by the Science Foundation Ireland under grant number 19/FFP/6485.

Notes and references

1 World Health Organization, Antimicrobial Resistance Fact Sheet, 2020.
2 L. A. Richardson, *PLoS Biol.*, 2017, **15**, e2003775.
3 World Health Organization, Lack of new antibiotics threatens global efforts to contain drug-resistant infections, Geneva, 2020.
4 D. J. Payne, M. N. Gwynn, D. J. Holmes and D. L. Pompliano, *Nat. Rev. Drug Discovery*, 2007, **6**, 29–40.
5 A. H. Holmes, L. S. P. Moore, A. Sundsfjord, M. Steinbakk, S. Regmi, A. Karkey, P. J. Guerin and L. J. V. Piddock, *Lancet*, 2016, **387**, 176–187.
6 C. Årdal, M. Balasegaram, R. Laxminarayan, D. McAdams, K. Outterson, J. H. Rex and N. Sumpradit, *Nat. Rev. Microbiol.*, 2020, **18**, 267–274.
7 S. Pushpakom, F. Iorio, P. A. Eyers, K. J. Escott, S. Hopper, A. Wells, A. Doig, T. Guilliams, J. Latimer, C. McNamee, A. Norris, P. Sanseau, D. Cavalla and M. Pirmohamed, *Nat. Rev. Drug Discovery*, 2019, **18**, 41–58.
8 E. J. Schulz, *Lepr. Rev.*, 1971, **42**, 178–187.

9 T. Yano, S. Kassovska-Bratinova, J. S. Teh, J. Winkler, K. Sullivan, A. Isaacs, N. M. Schechter and H. Rubin, *J. Biol. Chem.*, 2011, **286**, 10276–10287.
10 S. J. Yawalkar and W. Vischer, *Lepr. Rev.*, 1979, **50**, 135–144.
11 G. Bolla and A. Nangia, *Cryst. Growth Des.*, 2012, **12**, 6250–6259.
12 P. Bannigan, E. Durack, C. Madden, M. Lusi and S. P. Hudson, *ACS Omega*, 2017, **2**, 8969–8981.
13 C. K. Job, L. Yoder, R. R. Jacobson and R. C. Hastings, *J. Am. Acad. Dermatol.*, 1990, **23**, 236–241.
14 M. Murashov, J. Diaz-Espinosa, V. LaLone, J. Tan, R. Laza, X. Wang, K. Stringer and G. Rosania, *Pharmaceutics*, 2018, **10**, 238.
15 B. Lechartier and S. T. Cole, *Antimicrob. Agents Chemother.*, 2015, **59**, 4457–4463.
16 J. Lei, L. Sun, S. Huang, C. Zhu, P. Li, J. He, V. Mackey, D. H. Coy and Q. He, *Am. J. Transl. Res.*, 2019, **11**, 3919–3931.
17 J. M. Shin, J. W. Gwak, P. Kamarajan, J. C. Fenno, A. H. Rickard and Y. L. Kapila, *J. Appl. Microbiol.*, 2016, **120**, 1449–1465.
18 G. A. Dykes, R. E. W. Hancock and J. W. Hastings, *Biochem. Biophys. Res. Commun.*, 1998, **247**, 723–727.
19 F. J. M. van de Ven, H. W. van den Hooven, C. W. Hilbers and R. N. H. Konings, *Bacteriocins, Microcins and Lantibiotics*, Springer Berlin Heidelberg, Berlin, Heidelberg, 1992, pp. 435–447.
20 U. Jančič and S. Gorgieva, *Pharmaceutics*, 2021, **14**, 76.
21 A. A. T. Barbosa, M. R. de Melo, C. M. R. da Silva, S. Jain and S. S. Dolabella, *Crit. Rev. Microbiol.*, 2021, **47**, 376–385.
22 A. Lewies, J. F. Wentzel, A. Jordaan, C. Bezuidenhout and L. H. Du Plessis, *Int. J. Pharm.*, 2017, **526**, 244–253.
23 J. Flynn, A. Ryan and S. P. Hudson, *Eur. J. Pharm. Biopharm.*, 2021, **165**, 149–163.
24 S. Salmaso, N. Elvassore, A. Bertucco, A. Lante and P. Caliceti, *Int. J. Pharm.*, 2004, **287**, 163–173.
25 J. Flynn, S. Mallen, E. Durack, P. M. O'Connor and S. P. Hudson, *J. Colloid Interface Sci.*, 2019, **537**, 396–406.
26 J. Flynn, E. Durack, M. N. Collins and S. P. Hudson, *J. Mater. Chem. B*, 2020, **8**, 4029–4038.
27 N. Wang, J. Luo, F. Deng, Y. Huang and H. Zhou, *Front. Pharmacol.*, 2022, **13**, 839808.
28 S. Siddhaye, K. Camarda, M. Southard and E. Topp, *Comput. Chem. Eng.*, 2004, **28**, 425–434.
29 A. P. Singh, V. Prabha and P. Rishi, *PLoS One*, 2013, **8**, e76844.
30 S. Dosler and A. A. Gerceker, *Chemotherapy*, 2011, **57**, 511–516.
31 Q. Li, S. Yu, J. Han, J. Wu, L. You, X. Shi and S. Wang, *Food Chem.*, 2022, **380**, 132009.
32 W. Brumfitt, *J. Antimicrob. Chemother.*, 2002, **50**, 731–734.
33 K. Kitazaki, S. Koga, K. Nagatoshi, K. Kuwano, T. Zendo, J. Nakayama, K. Sonomoto, H. Ano and H. Katamoto, *J. Vet. Med. Sci.*, 2017, **79**, 1472–1479.
34 M. Hugo Silva, A. Kumar, B. K. Hodnett, L. Tajber, R. Holm and S. P. Hudson, *Cryst. Growth Des.*, 2022, **22**, 6056–6069.
35 C. R. Groom, I. J. Bruno, M. P. Lightfoot and S. C. Ward, *Acta Crystallogr., Sect. B: Struct. Sci., Cryst. Eng. Mater.*, 2016, **72**, 171–179.
36 CLSI, *M07: Dilution antimicrobial susceptibilty tests for aerobically grown Bacteria*, 11th edn, 2018.
37 J. Meletiadis, S. Pournaras, E. Roilides and T. J. Walsh, *Antimicrob. Agents Chemother.*, 2010, **54**, 602–609.
38 P. Ratrey, S. v Dalvi and A. Mishra, *ACS Omega*, 2020, **5**, 19004–19013.
39 K. A. Kristoffersen, A. van Amerongen, U. Böcker, D. Lindberg, S. G. Wubshet, H. de Vogel-van den Bosch, S. J. Horn and N. K. Afseth, *Sci. Rep.*, 2020, **10**, 7844.
40 H. Nie, Y. Su, M. Zhang, Y. Song, A. Leone, L. S. Taylor, P. J. Marsac, T. Li and S. R. Byrn, *Mol. Pharmaceutics*, 2016, **13**, 3964–3975.
41 P. Bannigan, J. Zeglinski, M. Lusi, J. O'Brien and S. P. Hudson, *Cryst. Growth Des.*, 2016, **16**, 7240–7250.
42 L. Migliore, A. Rotini and M. C. Thaller, *Dose-Response*, 2013, **11**, 550–557.
43 I. Castillo-Juárez, B. E. Blancas-Luciano, R. García-Contreras and A. M. Fernández-Presas, *PeerJ*, 2022, **10**, e12667.

